Optimization and Characterization of Friction Welded Joint between A6061 Tube Plate and ASTM A106 Grade B Steel Tube Using Taguchi Method

Sabu KT[1*], Amal V Purushothaman[2], Pradeep S[3], S Muthukumaran[4]

[1*,2,3,4]Department of Metallurgical and Materials Engineering, National Institute of Technology, Tiruchirappalli, India

***Corresponding author:** Sabu KT
*Email: sabuktitus@gmail.com

Abstract

Friction welding of tube to tube plate has gained momentum due to its ability to join dissimilar metals, particularly those that are difficult to weld using traditional welding techniques. This paper aims to explore the influence of major parameters like rotational speed of the tool, shoulder diameter, and feed rate on mechanical properties such as pull strength and microstructural features of A6061 aluminum alloy and ASTM A106 Grade B steel in which welds joined them. An optimal selection of parameters was obtained through Taguchi L9 orthogonal array to achieve maximum pull strength. Results indicated that 1400 rpm for the tool rotational speed with a shoulder diameter of 40mm and a feed rate of 1.2 mm/min gave rise to solid connections. At the interface between welds, SEM studies demonstrated refined grain structure without any intermetallic compounds indicating good bonding between two materials. The XRD analysis showed no formation of intermetallic phases as evidenced by uniform distribution of elements across the interface region confirmed by EDS results. These findings imply that the chosen process variables effectively increase joint strength and ensure a strong weld is formed in FWTPET processes, which could lead to improved industrial applications where high-performance joints for dissimilar metals are needed.

Keywords: FWTPET, Dissimilar joint, Pull strength, Taguchi technique, ANOVA.

Abbreviations

ANOVA	Analysis of variance
DOE	Design of Experiments
FWTPET	Friction welding of tube to tube plate using an external tool
S/N	Signal-to-Noise
DOF	Degree of freedom
SEM	Scanning Electron Microscopy
EDAX	Energy-dispersive X-ray spectroscopy
EBSD	Electron backscatter diffraction
XRD	X ray diffraction

1. Introduction

Friction welding is a solid-state welding technique that achieves a bond between metals by generating high-pressure frictional heat. It involves the relative motion and contact between two metal surfaces, resulting in the plasticization and subsequent bonding of the materials. This process is versatile and can join similar and dissimilar metals. Friction welding employs a non-consumable tool made of materials like tungsten carbide. The tool rotates along the joint line between the metal components, generating heat and pressure. This leads to the softening and intermixing of the metal, resulting in a solid-state weld without the need for melting. This approach offers advantages over conventional welding methods, as it can yield superior weld properties.
Friction welding of tube to tube plate using an external tool (FWTPET) was first invented by one of the authors of the manuscript in 2006, and a patent was granted in 2008[1]. This technique has gained considerable attention due to its many advantages, particularly its ability to join otherwise non-weldable alloys. In friction welding, heat is generated through frictional contact between the tool shoulder and the workpiece, resulting in plastic deformation and subsequent joining of the workpieces. FWTPET achieves a line joint interface similar to friction welding without any stir zone. Both workpieces are stationary in this process, and an external tool is employed to generate friction.
Aluminium alloys are extensively used in heat transfer, aerospace, and automobile industries due to their high corrosion resistance[2], low density, good formability[3], and high specific strength. However, welding aluminium using fusion welding techniques is challenging due to their high thermal conductivity[4]. Friction welding overcomes hot cracking[5], porosity[6], and alloy segregation[7] commonly encountered in fusion welding processes[8]. The material flow behaviour, microstructure and mechanical properties[9] of friction welded joints are directly influenced by process parameters. Researchers have focused on investigating the effects of axial force, transverse speed and rotational speed[10]. Traditional experimental techniques have

been commonly employed to study the influence of process parameters. However, these approaches require significant resources and are time-consuming. To overcome these challenges, many researchers have adopted a three level three factor design of experiments using Taguchi L9 orthogonal arrays, which allows for a relatively smaller number of experiments. Analysis of variance (ANOVA) and the Signal-to-Noise (S/N) ratio method has been utilized to identify the most significant process parameters and determine the overall contribution of each parameter. These statistical techniques enable researchers to study and optimize the friction welding process efficiently.

Pandiarajan et al.[11] friction welded SA 213 tube and SA387 tube plate using FWTPET process and optimized using Taguchi L9 array. It observed superior joint strength having process parameters as 1320 rpm, without tube projection and depth of cut of 0.2 mm. Karuppannaraja et al.[12] investigated the effect of compressive strength with and without a backing block using the Taguchi L9 array and found that a backing block has more compressive strength. SS Kumaran et al.[13] studied the effect of clearance and interference fit using a backing block arrangement. It observed that interference fit with the backing block shows higher joint strength.

This study aims to examine the influence of process parameters, namely tool rotational speed, tool shoulder diameter, and tool feed rate, on the formation of welds and the strength of joints. The primary aim is to identify the macrostructural and microstructural analyses of optimal parameters using scanning electron microscopy (SEM), energy-dispersive X-ray spectroscopy (EDAX) and electron backscatter diffraction (EBSD).These experimental techniques allow a comprehensive understanding of the weld quality, joint strength, and any occurrence of intermetallic phases in the FWTPET process.

2. Materials and methods

2.1 Selection of materials

In this experiment, a steel tube and A6061 plate were used as workpiece material. The chemical composition table is shown in Table 1

Table 1 Chemical composition of base materials

Base materials	Composition (wt. %)								
A6061		Mg	Si	Cu	Zn	Mn	Fe	Cr	Al
0.821	0.476	0.163	1.672	0.054	0.623	0.041	Bal		
ASTM A106		Si	S	P	Mn	C	Cr	Ni	Fe
Grade A		0.206	0.0074	0.0056	0.435	0.245	0.0204	0.0307	Bal

2.2 Method

Figure *1* illustrates the methodology followed in this research work

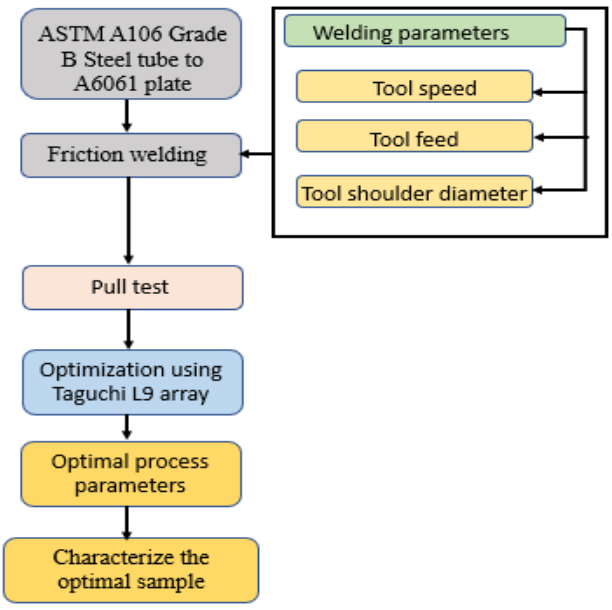

Figure 1

2.3 Work piece selection

The A6061 alloy plate was prepared with dimensions of 50 mm x 50 mm and a thickness of 10 mm. A hole with a diameter of 22 mm was drilled at the centre of the plate. The steel tube used in the experiment had a length of 30 mm, an outer diameter of 22 mm, and an inner diameter of 14 mm. Flash traps were created on the top part of the tube to enable bonding between the steel and aluminium. These flash traps comprised two rows of 2.0 mm diameter holes, equally spaced 1 mm from the edge. To ensure stability during welding, samples were welded using a backing block. Figure 2 provides a cross sectional view of the workpiece and illustrates the tool and backing plate in position.

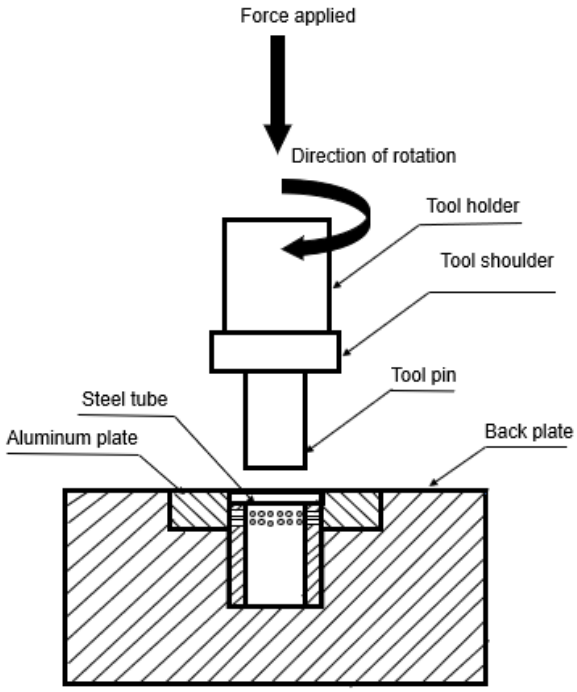

Figure 2 Experimental setup

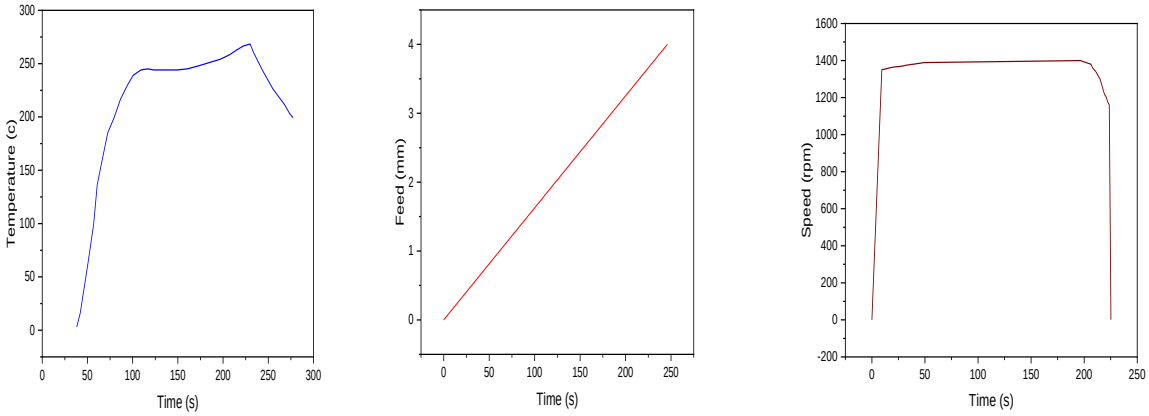

Figure 3 Dependence of welding parameters

The quality of the friction welded joint is influenced by four significant parameters namely tool speed, tool feed, tool temperature, and friction time. Tool speed controls the level of plastic deformation that takes place during the process. Tool shoulder diameter affects the temperature obtained due to friction, while friction time determines the duration for which the surfaces are heated to the maximum temperature. It is crucial to select the optimal values for these parameters to achieve favourable results and obtain a well formed friction welded joint. Figure 3 shows the complete dependence of the welding parameters on time, which has been determined based on existing literature, experimental trials, and practical experience in the field.

3. Experimental procedure

3.1 FWTPET process

The setup for friction welding is demonstrated in Figure 2. The setup involves fixing the aluminium alloy plates 6061 and the ASTM A106 grade B steel tube with an interference fit onto the table using fixtures. A range of controllable parameters were selected based on trial experiments, as delineated in Table 2. The welding process followed an L9 orthogonal array design, as shown in Table 3, which helps reduce the effort and cost of experimentation. Three external tools were obtained for this investigation, each with a shoulder diameter of 35 mm, 40 mm, and 45 mm and a pin diameter of 14 mm. Prior to assembly, the surface of the tube and plate was cleaned with acetone. During assembly, the tube tip was positioned 5 mm below the top surface of the plate. A backing plate was fixed onto the machine table to provide stability. A sequence of experiments was performed to optimize the process parameters. The machine's spindle was set to the desired rotational speed, and the tool post containing the external tool was lowered to create contact with the workpiece. Upon contact, the frictional force generated heat and caused plasticization of the metal, resulting in the flow of metal into the flash traps. Filling the flash traps enabled the locking of the tube and plate, forming the joint. The tool's pin and shoulder controlled the metal flow into the flash traps. The investigation was repeated for different parameters, as specified in Table 3.

3.2 Pull test

Pull tests were conducted to evaluate the material's response and ability to withstand shear loads. The pull testing was conducted with a universal testing machine. One side of the jaw was fixed to the steel tube, while a specially fabricated fixture was bolted to the A6061 plate to fix the other side. The force was applied parallel to the axis of the tube, inducing shear stress on the joint.

Table 1: Friction welding input parameters and their different level with DOF

Parameter	Unit	Levels			DOF
		I	II	III	
Tool rotational speed	rpm	1120	1400	1800	2
Tool feed	mm/min	0.8	1.0	1.2	2
Tool shoulder diameter	mm	35	40	45	2
Total DOF					6

3.3 Microstructural study

For finding the micrograph, the joint was cut using wire cut EDM then the samples were ground on 220, 320, 400, 600, 800, 1000,1200, and 2000 grid silicon carbide abrasive sheets. The samples were completely washed, dried, and polished to produce a good surface finish. The A6061 alloy side of polished samples was then etched for 20 seconds using Modified Keller’s reagent solution, and the steel part using nital to obtain the macrostructure and microstructure.

4. Results and discussion

4.1. Taguchi analysis

4.1.1. Design of experiments

The branch of statistics deals with planning, gathering, and experimental data to ensure valid conclusions to solve engineering problems using numerous techniques and principles to ensure the availability of sound, encouraging, and cogent results is called the design of experiments[14] (DOE). It was first introduced by Fisher[15], who developed the concepts of randomization, blocking, replication, factorial approach, and analysis of variance[16]. DOE deals with knowing the effect of independent variables on the depended variables[17]. The primary aim is to obtain optimized results with the least data.

4.1.2. Statistical analysis techniques

Analysis of Variance (ANOVA) and the Taguchi method is the important analysis technique used in this work. ANOVA technique is used to assess any deviation related to the main effects within the design and separate it from the independent variables, which are distinct with three or more levels. It utilises the least squares method to find the cause of variation within a dataset. For applying ANOVA, the following assumptions should be satisfied. Every replicate should be independent of all others, and experimental measurements should be entirely randomized. The probability value (p-value), a measurement of the likelihood that any identified difference could have happened by random chance, confirms the confidence level of the ANOVA. The null

hypothesis can be rejected when the p-values are too little, often set at 0.05. which indicates that there is a statistically significant difference between group means. The higher the F value, the smaller the p- value.

4.1.3. Taguchi method

A loss function proposed by Genichi Taguchi[18] evaluates the disparity between the desired target and experimental values. This loss function is then transformed into a signal-to-noise (S/N) ratio, widely used in electrical, electronic, and communication engineering fields. In these domains, maximising amplifier output while minimizing noise is crucial. The S/N ratio represents the relationship between the mean and standard deviation of measured values and indicates parameter variation under noisy conditions. A higher deviation from the target value indicates a greater decline in quality.

Taguchi categorized the S/N ratio into three groups, lower is better, medium is better, and higher is better, depending on the desired response characteristic. The appropriate categorization depends on the specific response characteristic being sought. For instance, in the current investigation, when aiming for a stronger response characteristic such as pull strength, a higher S/N ratio is necessary to enhance shear strength. The calculation of the S/N ratio utilizes Equation (1).

Signal to noise ratio for the larger the better = -10 $\left[log\left(\sum\left(\frac{1}{y2}\right)/n\right)\right]$ (1)

In the equation n represents the number of observations while y refers to the observed data corresponding to each response.

4.1.4. Effect of process parameters on pull strength

The impact of process factors on pull strength is shown in Table 3. Increasing the tool speed has been observed to result in higher pull strength. This can be attributed to increased friction between the tool and workpiece, generating more heat. As a result, the workpiece experiences greater plastic deformation and flows into the flash traps of the steel tube. The effect of each parameter on pull strength was investigated in this study. A specific parameter was set to a designated level to obtain this result, and the corresponding pull strength value was subtracted from the overall mean.

$$Pd = \frac{1}{n}\sum_{j=1}^{n} yj - \bar{y}o \quad (2)$$

Where Pd represents the effect of a specific parameter and n refers to the number of experiments

4.1.5. Prediction of responses

The optimized responses can be determined by considering the impact of each parameter on the responses, in addition to the overall mean and the S/N ratio. The mathematical expression used to predict the responses is as follows:

$$Y_{predicted} = \bar{k}o + \sum \mathrm{Pe} + \sum \mathrm{Ie} + \varepsilon \quad (3)$$

Where $\bar{k}o$ represents the overall mean of the responses or the S/N ratio. Pe denotes the effects of the parameters on the responses, while Ie signifies the interaction effect of the responses and ε represents the statistical error associated with the model. In this Taguchi approach, the interaction effect of the responses and statistical errors are not taken into account. Therefore, the equation for predicting the responses becomes

$$Y_{predicted} = \bar{k}o + \sum \mathrm{Pe} \quad (4)$$

4.1.6. Effect of process parameters on pull strength

Pull strength is influenced by process parameters, as shown in Table 3. It has been found that pull strength increases as the tool speed increases from 1120 rpm to 1400 rpm. As the tool's speed increases, there is an increase in friction between the tool and the workpiece, which raises the temperature and causes the A6061 alloy to plasticize, allowing the metal to extrude to the drilled hole of steel pipe and resulting in sound welding. The tool speed increases from 1400 mm to 1800rpm friction heat increases, and higher temperature promotes grain growth, resulting in reduced strength due to coarse grain structure.

Table 2: Pull strength of the specimen with the combination of process parameters

Sl No	Tool rotation Speed (s) (Rpm)	Tool shoulder Diameter (d) (mm)	Tool feed (f) (mm/min)	Pull strength (MPa)	SN ratio of the result
1	1120	35	0.8	43.3	32.72
2	1120	40	1.0	45.4	33.14
3	1120	45	1.2	47.3	33.49
4	1400	35	1.0	83.2	38.40
5	1400	40	1.2	85.4	38.62
6	1400	45	0.8	82.7	38.35
7	1800	35	1.2	72.2	37.17
8	1800	40	0.8	74.3	37.41
9	1800	45	1.0	73.8	37.36

Table 3: Response Table for Means

Level	Tool speed	Tool Shoulder diameter	Tool feed
1	45.33	66.23	66.77
2	83.77	68.37	67.47
3	73.43	67.93	68.30
Delta	38.43	2.13	1.53
Rank	1	2	3

Table 4: Response Table for Signal to Noise Ratios

Level	Tool speed	Tool Shoulder diameter	Tool feed
1	33.12	36.10	36.17
2	38.46	36.40	36.30
3	37.32	36.40	36.43
Delta	5.34	0.30	0.27
Rank	1	2	3

4.1.7. Signal to noise ratio.

The investigation aimed to achieve good pull strength by utilizing a properly welded FWTPET joint. Minitab software was employed to calculate the mean and SN ratio, allowing for the evaluation of the influence of each factor on the response. The criterion of larger is better was considered in selecting the SN ratio. The response tables for means and signal to noise ratio are provided in Tables 4 and 5, respectively.

4.1.8. Microstructural and Compositional Analysis

The characterization of the friction welded joint was prepared according to the optimized welding parameters conditions of 40 mm shoulder diameter, 1400 rpm, and 1.2mm/min tool feed rate. After welding, the specimens were carefully prepared, including polishing and etching, to reveal the microstructural details.

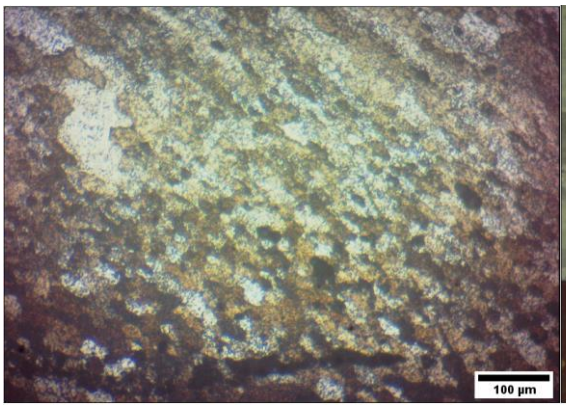

Figure 4. Micrograph of Aluminium

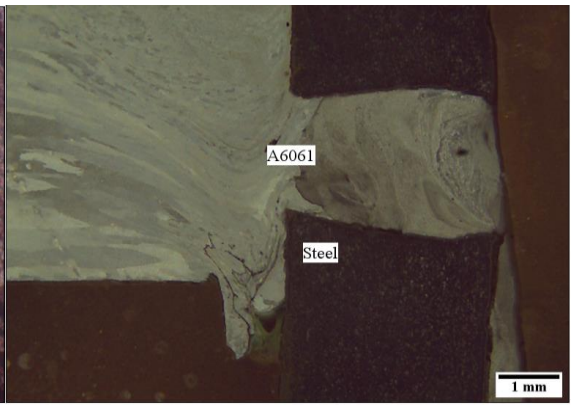

Figure 5 Macrograph of the joint

Figure 4 shows the micrograph after friction welding in the A6061 plate. The macrograph of the A6061 plate and ASTM 106 steel tube welded with the same parameters is shown in Figure 5. The figure shows that the A6061 alloy plate is plastically deformed and filled into the flash traps of steel tube and resulting in a good bond.

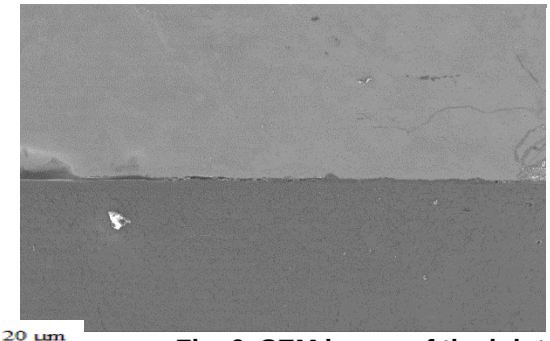

Fig. 6. SEM image of the joint

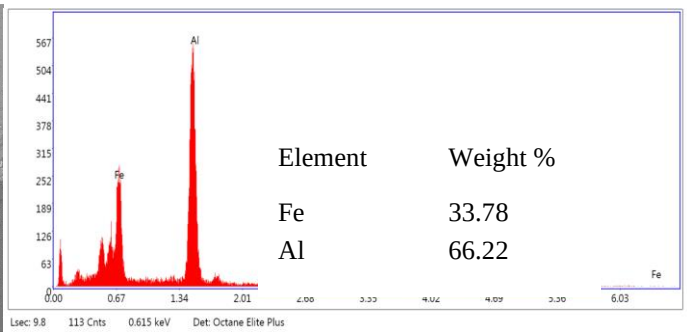

Fig. 7 EDS results of the joint

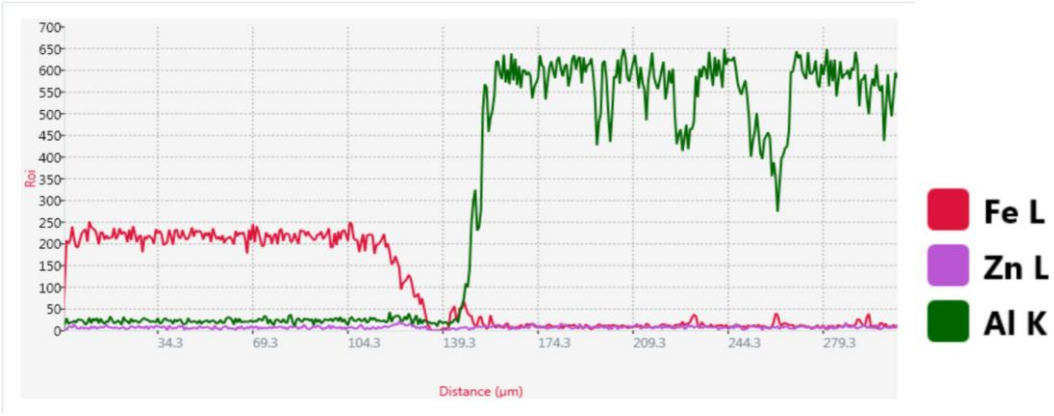

Figure 8 Line scan of the joint

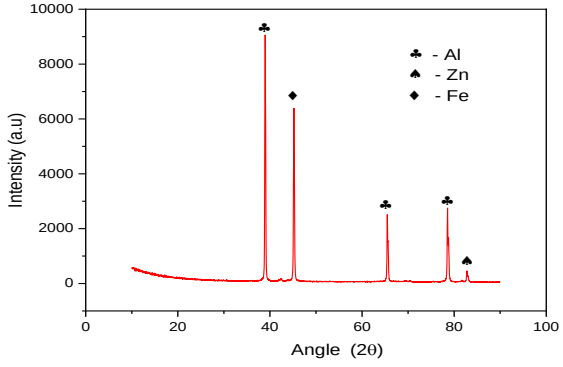

Fig. 9 XRD result of the joint

In Figure 7, The SEM analysis was performed to investigate the microstructure of the joint. It involved capturing images to observe grain structure, interfacial bonding, and defects like voids, cracks, or intermetallic phases. Figure 8 shows the EDS line analysis of Fe and Al elements corresponding to the interface of the FWTPET joint. EDAX was conducted to find the elemental composition of the weld. This analytical technique involves subjecting the sample's surface to an electron beam, which causes the elements within the sample to emit characteristic X-rays. By detecting and analyzing these emitted X-rays, the elemental composition of the joint can be determined. Analysing the X-ray spectrum makes it possible to determine the elemental composition and distribution across the joint interface. The elemental mapping revealed a uniform distribution of elements across the joint interface, indicating a successful fusion between the two materials. The absence of intermetallic phases or composition variations suggested a compatible weld interface. This is significant as intermetallic compounds at the interface of dissimilar materials can negatively affect the joint's mechanical properties. The EDS analysis revealed the chemical compositions at the interface, with Fe constituting 33.78% and Al making up 66.22% of the material. Fig. 9 shows the results of the XRD analysis of the interface between Al/Fe. Notably, no intermetallic compounds were observed in this region. The absence of intermetallic compounds suggests a favourable bonding and absence of adverse interactions between Al and Fe during the FWTPET process.

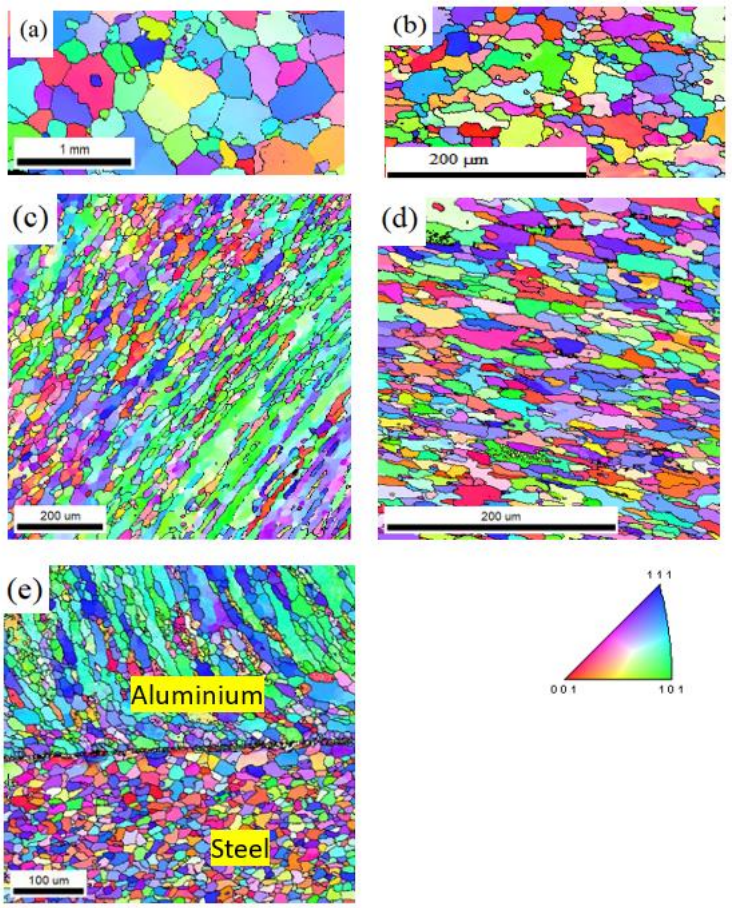

Figure 10 EBSD map of (a) A6061 base metal (b) ASTM A106 Grade B steel (c) after FWTPET on Al side (d) after FWTPET on Fe side (e) Interface of the joint.

EBSD analysis provided valuable information about the joint's grain orientations and texture evolution. The crystallographic orientations of individual grains could be mapped and analysed to understand the distribution of preferred orientations and potential texture development during the welding process. The EBSD analysis revealed the microstructural features of the joint, including the presence of distinct grain structures and grain boundaries. Fig. 10(a) and Fig. 10(c) displays the IPF maps of the material before and after undergoing FWTPET on aluminium side. The base metal had an average grain size of 125.2 µm with an equiaxed grain structure. A few bulges were observed along the grain boundaries, typically caused by the varying strain accommodation in neighbouring grains. In order to release stored energy, the grain boundaries tend to migrate from low strained grains to high strained grains. The severe plastic deformation during the FWTPET process resulted in the accumulation of dislocations, leading to the formation of dislocation cells. These cells could eventually transform into low angle grain boundaries or even high angle grain boundaries. The region depicted in figures 10(b) and 10(d) shows the IPF maps of the steel side before and after FWTPET. It did not

experienced a higher degree of plastic deformation. In this region, the microstructure primarily consisted of elongated grains and a smaller proportion of equiaxed grains that exhibited reduced size. A notable transformation occurred in the grain boundaries of the material as the strain increased. Initially, the material exhibited low-angle grain boundaries, which indicates a relatively small misorientation between adjacent grains.

Figure 10(e) presents the inverse pole figure (IPF) map in the interface region between Al and steel. The microstructure at the interface is characterized by lamellar-like shear bands, which are predominantly composed of Al. These shear bands form due to the deformation and mixing of the two dissimilar materials during the FWTPET process. The microstructure exhibits intricate and intercalated flow patterns, similar to what has been observed in other dissimilar friction welding joints. These flow patterns are a result of the complex interaction and deformation occurring between the two materials as they are subjected to the FWTPET process, leading to the formation of the final joint at the interface. A significantly refined grain structure is evident on the upper surface, with an average grain size of 14.2µm, considerably smaller than the base metal. This microstructural refinement in the upper surface is attributed to dynamic recrystallization, a process that promotes the formation of new, smaller grains during deformation. Since the rotating tools used in the FWTPET process did not penetrate the lower steel, the overall plastic deformation of the steel was minimal. Consequently, no noticeable difference was observed in the final microstructure of the steel.

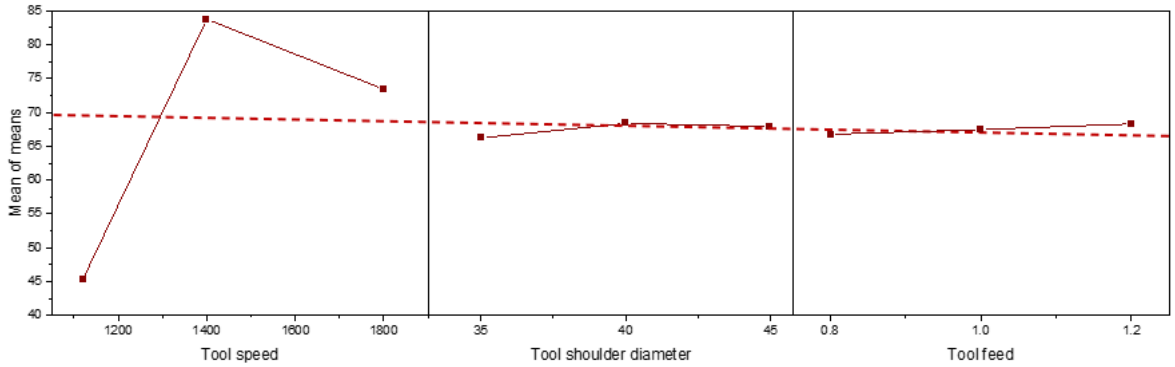

Figure 11 Main effects plot for means

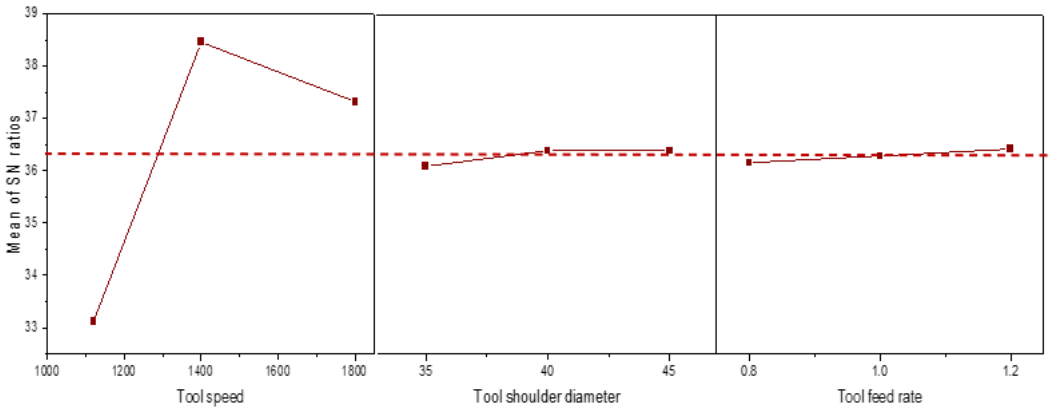

Figure 12 Main effects plot for SN ratios

4.1.9. Selection of optimum friction welding condition

The main effects plots for the S/N ratio graph and the mean effects plots for means are shown in Figure 11 and Figure 12, respectively. The S/N ratio is larger when the difference between the measured and preferred outputs is as small as possible. Figure 11 shows that the higher mean S/N ratio attained for pull strength is shoulder diameter of 40mm, speed of 1400 rpm, and feed rate of 1.2mm per minute.

4.1.10. ANOVA for pull strength

The process parameter that has the biggest impact on the performance characteristics is shown using ANOVA. The results of the pull test using ANOVA are shown in Table 6.

Table 6: Result obtained from ANOVA

Source	DF	Seq.SS	Adj.MS	F value	P Value	% Contri-bution
Tool speed	2	2373.51	1186.75	703.15	0.001	99.39
Tool shoulder dia.	2	7.63	3.81	2.26	0.307	0.32
Tool feed	2	3.54	1.77	1.05	0.488	0.15
Error	2	3.38	1.69			0.14
Total	8	2388.05				100.00

The process parameter that has the biggest impact on the performance characteristics is shown using ANOVA. The results of the pull test using ANOVA are shown in Table 6. The R^2 [19] coefficient of determination was used to confirm the model's capacity. The coefficient of determination has a value that ranges from zero to one. If the value is close to one, the dependent variable and independent variable suit each other well. This study's generated regression model for pull strength has an estimated high level of variability at 99.86 percent R^2. It was noted that there is good agreement between the experimental findings and the model's expected outcomes and the supplied parameters. In the literature on material machining,[20] similar correlations between the process parameters and reaction could be discovered.

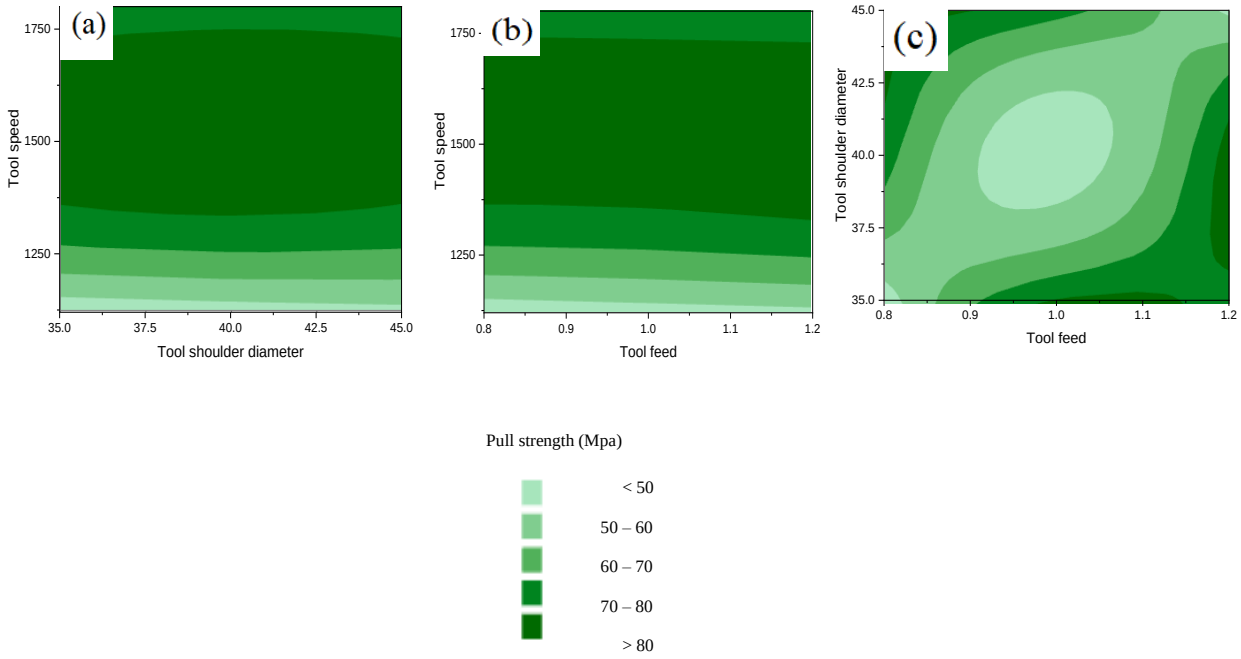

Figure 13(a) Contour plot of pull strength vs tool speed, tool shoulder diameter, Figure 13(b) Contour plot pull strength vs Tool speed, Tool feed, Figure 13(c) Contour plot of pull strength vs tool shoulder diameter , tool feed.

Figure 13 illustrates the contour plots that describe the connection between process parameters and pull strength. It observed that tool rotation speed between 1375rpm and 1700 rpm have good pull strength irrespective of tool shoulder diameter and feed rate. From **Error! Reference source not found.**13(c) it was obtained that higher tool shoulder diameter and low tool feed rate result in higher pull strength and moderate tool shoulder diameter and higher tool feed rate also results in higher pull strength. Similar kind of effects was observed in the optimization of TIG welding parameters[21].

Conclusion

1. The dissimilar metals ASTM A106 Grade B tube and A6061 alloy plate had welded successfully by FWTPET process.
2. It found that the most significant parameter in determining the joint strength is found tool speed of 1400 rpm

3. The analysis of variance computed tool speed as the highest percentage of contribution at 99.39% which is followed by tool shoulder diameter at 0.32% and tool feed at 0.15%.
4. SEM, EBSD and XRD provide insights into grain structures, texture development, and elemental composition, confirming the absence of intermetallic compounds.

References

1. S. Muthukumaran: Process for friction welding tube to a tube sheet or plate by adopting an external tool, Indian patent 21744. (2008)., (2008)
2. Islam, S., Sakairi, M.: Corrosion behavior of A6061 aluminum alloy in cation containing aqueous medium. Corrosion Communications. 5, 39–48 (2022). https://doi.org/10.1016/j.corcom.2022.01.001
3. Meng, Y., Sugiyama, S., Tan, J., Yanagimoto, J.: Effects of forming conditions on homogeneity of microstructure and mechanical properties of A6061 aluminum alloy manufactured by time-dependent rheoforging on a mechanical servo press. Journal of Materials Processing Technology. 214, 3037–3047 (2014). https://doi.org/10.1016/j.jmatprotec.2014.07.014
4. Seli, H., Ismail, A.I.M., Rachman, E., Ahmad, Z.A.: Mechanical evaluation and thermal modelling of friction welding of mild steel and aluminium. Journal of Materials Processing Technology. 210, 1209–1216 (2010). https://doi.org/10.1016/j.jmatprotec.2010.03.007
5. Li, H., Yan, W., Li, Z., Mariusz, B., Senkara, J., Zhang, Y.: Numerical and experimental study of the hot cracking phenomena in 6061/7075 dissimilar aluminum alloy resistance spot welding. Journal of Manufacturing Processes. 77, 794–808 (2022). https://doi.org/10.1016/j.jmapro.2022.04.001
6. Liu, B., Wang, C., Mi, G., Wang, J., Zhang, W., Zhang, X.: Oxygen content and morphology of laser cleaned 5083 aluminum alloy and its influences on weld porosity. Optics and Laser Technology. 140, 107031 (2021). https://doi.org/10.1016/j.optlastec.2021.107031
7. Kawakubo, T., Ushioda, K., Fujii, H.: Grain boundary segregation and toughness of friction-stir-welded high-phosphorus weathering steel. Materials Science and Engineering: A. 832, 142350 (2022). https://doi.org/10.1016/j.msea.2021.142350
8. Soysal, T., Kou, S., Tat, D., Pasang, T.: Acta Materialia Macrosegregation in dissimilar-metal fusion welding. Acta Materialia. 110, 149–160 (2016). https://doi.org/10.1016/j.actamat.2016.03.004
9. Luo, Q., Yin, L., Simpson, T.W., Beese, A.M.: Effect of processing parameters on pore structures, grain features, and mechanical properties in Ti-6Al-4V by laser powder bed fusion. Additive Manufacturing. 56, 102915 (2022). https://doi.org/10.1016/j.addma.2022.102915
10. Lin, Y.C., Chen, J.N.: Influence of process parameters on friction stir spot welded aluminum joints by various threaded tools. Journal of Materials Processing Technology. 225, 347–356 (2015). https://doi.org/10.1016/j.jmatprotec.2015.06.024
11. Pandiarajan, S., Senthil Kumaran, S., Kumaraswamidhas, L.A., Saravanan, R.: Interfacial microstructure and optimization of friction welding by Taguchi and ANOVA method on SA 213 tube to SA 387 tube plate without backing block using an external tool. Journal of Alloys and Compounds. 654, 534–545 (2016). https://doi.org/10.1016/j.jallcom.2015.09.152
12. KaruppannaRaja, P.G., Rajkumar, M., S., S.K.: A study on backing block arrangement of dissimilar metal joining process of seamless ferritic and austenitic alloy by using an external tool. Journal of Alloys and Compounds. 687, 773–785 (2016). https://doi.org/10.1016/j.jallcom.2016.06.195
13. Senthil Kumaran, S., Daniel Das, A.: Friction Welding Joints of SA 213 Tube to SA 387 Tube Plate Boiler Grade Materials by using Clearance and Interference Fit Method. Materials Today: Proceedings. 5, 8557–8566 (2018). https://doi.org/10.1016/j.matpr.2017.11.553
14. Thomas P. Ryan: Statistical Methods for Quality Improvement. John Wiley & Sons, Inc. (2011)
15. Fisher, R.A. (1960).: The Design of Experiments. HAFNER PRESS (1937)
16. Cox, D. R., & Reid, N.: The theory of the design of experiments. CRC Press. (2000)
17. Mongomery, D.C., M.: Design and Analysis of Experiments. John Willy & Sons. (2017)
18. Imsap, N., Luangpaiboon, P.: A Comparative Study of Analysing Transformed and Noisy Data in Taguchi Orthogonal Arrays. II, (2015)
19. Gupta, M.K., Sood, P.K., Sharma, V.S.: Machining Parameters Optimization of Titanium Alloy using Response Surface Methodology and Particle Swarm Optimization under Minimum-Quantity Lubrication Environment. Materials and Manufacturing Processes. 31, 1671–1682 (2016). https://doi.org/10.1080/10426914.2015.1117632
20. Gupta, M.K., Sood, P.K., Singh, G., Sharma, V.S.: Sustainable machining of aerospace material – Ti (grade-2) alloy: Modeling and optimization. Journal of Cleaner Production. 147, 614–627 (2017). https://doi.org/10.1016/j.jclepro.2017.01.133
21. Juang, S.C., Tarng, Y.S.: Process parameter selection for optimizing the weld pool geometry in the tungsten inert gas welding of stainless steel. Journal of Materials Processing Technology. 122, 33–37 (2002). https://doi.org/10.1016/S0924-0136(02)00021-3

DOI: https://doi.org/10.15379/ijmst.v10i1.3816